High Heat Flow in the Idaho Thrust Belt: A Hot Sedimentary Geothermal Prospect

John Welhan[1] and Mark Gwynn[2]

[1]Idaho Geological Survey, Idaho State University, Pocatello, ID
[2]Utah Geological Survey, Salt Lake City, UT

Keywords

Heat flow, hot sedimentary basin, magmatic-hydrothermal, thermal conductivity, bottom-hole temperature

ABSTRACT

A synthesis of bottom-hole temperature (BHT) and drill stem test (DST) data compiled for the National Geothermal Data System (NGDS) in the vicinity of southeast Idaho's Blackfoot volcanic field (BVF) was used to calculate heat flow for 31 oil and gas exploration wells drilled in the Idaho thrust belt (ITB). The temperature data and heat flow estimates define a previously unrecognized high-temperature geothermal prospect in Jurassic and Triassic sedimentary rocks adjacent to the BVF at depths of 3–4 km, approximately 25–50 km north of the late Quaternary (58 ka) China Hat rhyolite domes of the BVF. The rhyolite magma, at a depth of 12–14 km, and/or its associated parent mafic magma is believed to be the heat source responsible for driving hydrothermal fluids and heat into the ITB.

Several BHT correction methods were tested against DST data and an aggregate average of the best methods was computed and applied to all BHT data. Formation thermal conductivities were also evaluated to calculate more accurate heat flow. An area greater than 150 km² has heat flow greater than 120 mW/m^2 and temperatures in excess of 150ºC at 3 km. Another localized area defined by a single well also exhibits anomalously high heat flow and subsurface temperatures (116 mW/m^2 and 170ºC at 3.5 km, respectively).

The major ion chemistry of hot brines and saline formation fluids indicates they are the product of dissolution of evaporite beds in the Jurassic Preuss Sandstone in response to circulating hydrothermal fluids. Their spatial occurrence relative to salt-bearing strata suggests they may play a role in redistributing and storing heat, which could have implications for how these hot sedimentary reservoirs are developed.

1. Introduction

The Blackfoot Reservoir - Gray's Lake area of southeast Idaho, in which the Blackfoot Volcanic Field (BVF) is found (Figure 1), was once considered "one of the most favorable geothermal prospects in Idaho" (IDWR, 1980; Mitchell et al., 1980). Very young rhyolite domes in the China Hat graben are believed to represent a considerable high-temperature thermal mass at depth (McCurry

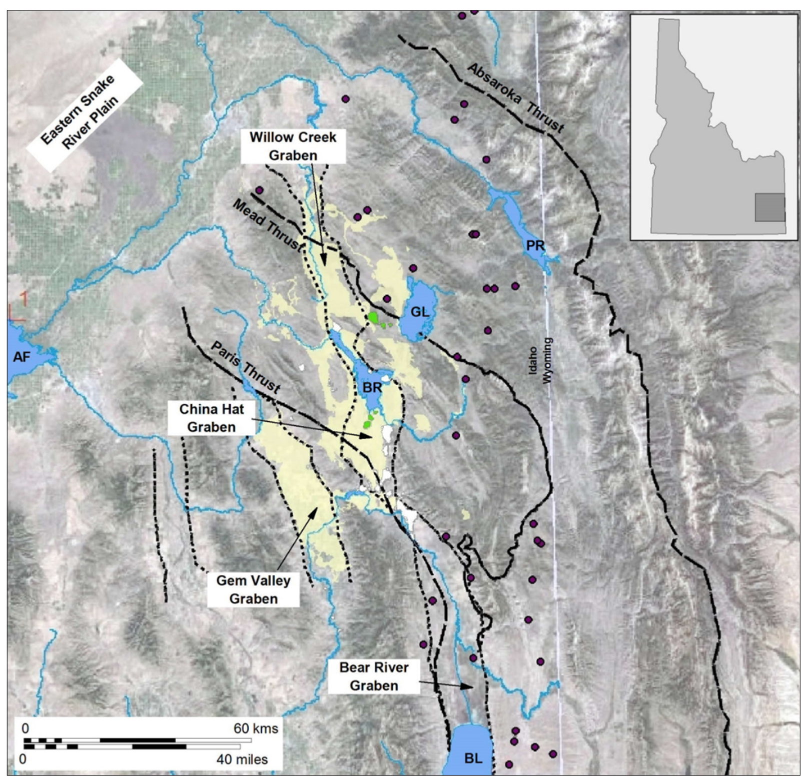

Figure 1. Location of the study area showing the Blackfoot volcanic field's basalt-filled grabens (tan), major thrust faults (heavy dashed lines) and Basin and Range grabens (light dashes). Travertine deposits are shown in white and deep oil and gas wells are shown as filled circles. Abbreviations: AF = American Falls reservoir; BR = Blackfoot Reservoir; PR = Palisades Reservoir; BL = Bear Lake; GL = Gray's Lake.

and Welhan, 2012) whose residual thermal energy was estimated at 7 x 10^{10} MW_t -hours, equivalent to that of the Newberry Crater resource (Smith and Shaw, 1979).

Although a lack of evidence for a high-temperature resource has led to speculation that the magma chamber may have been too small to retain significant heat, evidence presented by McCurry and Welhan (2012) indicates that this cannot be correct.

The fact that the China Hat domes are typical topaz rhyolites (Ford, 2005) and the product of extreme fractional crystallization (e.g., Christiansen et al, 1986) further supports the hypothesis that a large mass of unerupted magma remains at a depth of ca. 15 km. Furthermore, Lewicki et al. (2012) provided unequivocal evidence that magmatic volatiles are actively outgassing from beneath the southern BVF.

If a considerable volume of hot magma is present, then why is the heat not expressed within the China Hat graben? Other than a few warm springs (T_{max} = 40ºC) and large travertine deposits (Figure 1), there are no high-temperature manifestations. A 2.36-km-deep geothermal exploratory well drilled just south of the China Hat rhyolite domes encountered a bottom-hole temperature (BHT) of only 69 ºC (NGDS, 2012). Welhan et al. (2013; 2014) proposed that heat from the magma may be diverted laterally along regional thrust structures, providing pathways for hydrothermal fluids originating in the vicinity of the magmatic heat source to rise into the adjacent Idaho thrust belt (ITB).

1.1. Objectives

The objectives of this paper are to (1) perform a second-order assessment of BHT, lithology, and drill stem test (DST) data from 31 exploration wells in the ITB to improve heat flow estimates, (2) evaluate lithologic variations and refine thermal conductivity estimates, and (3) define the depths to target temperatures (> 150ºC) that have been identified as economic in these types of sedimentary rocks (Allis et al., 2013; Allis and Moore, 2014). In addition, we examine an hypothesis posed by Welhan et al. (2013, 2014) concerning the role that hot brines may play in storing heat in the sedimentary section.

1.2. Geologic and Geothermal Setting

The BVF is a Quaternary-age bimodal complex of basalt lava flows and rhyolite domes in the northeastern-most part of the Basin and Range (B&R) Province where it transitions into the ITB (Figure 1) south of the eastern Snake River Plain's (ESRP) southern margin. Between about 1.5 and 0.06 Ma, three major B&R grabens as well as adjacent topographic lows received more than 50 km^3 of basalt over a 1350 km^2 area.

The crustal framework comprises ca. 40 km of Archean to early Proterozoic crust overlain by 6–10 km of late Proterozoic to Mesozoic carbonate and clastic rocks. Pre-Cretaceous rocks, predominantly limestone, dolomite, shale and quartz sandstone, have a total conformable thickness of approximately 7300 m. During Laramide, Sevier and older orogenies, these rocks were stacked eastward in large thrust sheets (Armstrong and Oriel, 1965; Royse, 1993). Up to several hundred meters of Miocene to Pliocene silicic tuffs, tuffaceous sediments and lacustrine deposits of the Salt Lake Formation underlie the basalt lavas of the BVF (Armstrong, 1969).

B&R normal faulting began in the mid-Miocene in response to east-west extension and interaction with the Yellowstone-ESRP hot spot track, followed by filling of the Willow Creek-China Hat and Gem Valley grabens starting in late Pliocene (McCurry and Welhan, 2012). The China Hat rhyolite domes erupted from a depth of 12–14 km, as constrained by hornblende thermobarometry (Ford, 2005). Recent work on the flux of CO_2 in the southern BVF has demonstrated that as much as 350 tons/day emanate via warm springs and soil (Lewicki et al. 2012), comparable to CO_2 emission rates associated with active quiescent volcanoes. Lewicki et al. also found elevated $^3He/^4He$ ratios (1.8-2.4 R_a), confirming that a significant fraction of this volatile flux is of magmatic origin.

Figure 2 summarizes the stratigraphic column in the study area. Many of the sedimentary formations known to be productive oil and gas reservoirs in the northern Utah thrust belt are also known to host the largest ground water flows in the upper km of the study area, namely: the fractured limestone of the Pennsylvanian Wells formation; the fractured limestones and siltstones of the Triassic Dinwoody Formation and fractured limestone of the Thaynes Formation; and the Jurassic Stump and Nugget Sandstones and the Twin Creek Limestone (Ralston and Williams, 1979; Ralston et al., 1983; Ralston and Mayo, 1983).

Until recently, few reliable heat flow estimates were available in the study area and the majority of shallow-well estimates reflect advective overprinting by shallow ground water. Of 38 wells in Southern Methodist University's (SMU's) heat flow database that are located in and around the BVF, fourteen are classified as having reliable information but only seven have associated heat flow estimates (SMU, 2008). Several shallow wells with BHTs < 16 ºC have heat flows ranging from 28 to 51 mW/m^2, but four locations exceed 120 mW/m^2, including a 2900-meter wildcat petroleum well east of the BVF, and heat flows of 138 to 167 mW/m^2 are reported in the area of magmatic outgassing identified by Lewicki et al. (2012). Heat flow in the northern B&R Province is generally in the range of 80–100 mW/m^2 (Blackwell, 1983; Lachenbruch et al., 1994; Henrikson and Chapman, 2002). The regional heat flow map of Blackwell and coworkers (2011) indicates that the highest heat flow in the ITB occurs north of the China Hat rhyolite domes, well outside the China Hat graben.

Based on corrected BHT data for 20 deep exploration wells, Welhan et al. (2014) estimated thermal gradients and approximate heat flows of less than 80 mW/m^2 in the China Hat and Bear River grabens. A zone of elevated heat flow extends over a wide area to the east of the China Hat grabens, ranging from ca. 80 mW/m^2 in the vicinity of Bear Lake to >120 mW/m^2 north-northeast of the rhyolite domes. As Welhan et al. (2013, 2014) pointed out, hot sodium-chloride brines occur at depths of 2–5 km within the zone of elevated heat flow and are apparently derived from dissolution of evaporite minerals in the salt-bearing interval of the Jurassic Preuss Sandstone and from minor evaporites throughout the stratigraphic section.

2. Data Sources

Historic petroleum well drilling in the ITB has provided considerable information on the area's stratigraphy, structure, and geothermal potential. Data from 30 deep petroleum exploration wells and a 2.4-km-deep geothermal exploration well drilled in the study area have provided considerable information on formation tops, temperatures, heat flow, and geothermal fluid composition (NGDS, 2012; Welhan et al., 2013, 2014).

2.1. Lithology and Structure

Figure 3 depicts typical cross sections across the study area showing the stratigraphic and structural context of selected petroleum exploration wells. These cross sections represent structurally balanced reconstructions by Dixon (1982) based on a synthesis of hundreds of seismic line miles and hundreds of deep wells throughout the Idaho-Utah-Wyoming thrust belt. Key stratigraphic units known to host productive oil and gas reservoirs in the northern Utah thrust belt are plotted for reference based on formation tops data (NGDS, 2012); the Jurassic Preuss Sandstone is also shown because of its role in brine formation (Section 4.2).

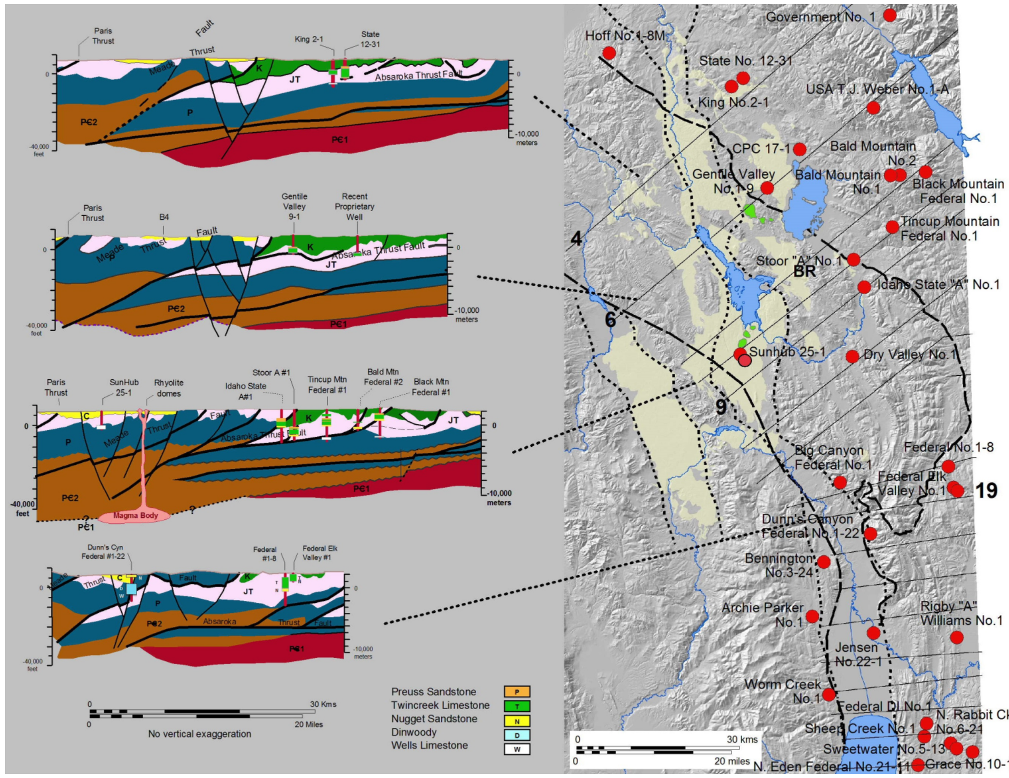

Figure 3. Oil and gas exploration wells whose data were used to compile this analysis of heat flow and geothermal fluids. Cross sections are from Dixon (1982), representing structurally balanced reconstructions of ITB structure and stratigraphy.

2.2. Temperature Data

Almost 50 oil exploration wells have been drilled in the study area and data for these can be found on the Idaho Geological Survey's website[1]. Of these, 29 wells drilled from the 1950s to the 1980s were found to have geophysical logs with temperature data. DST data were also available for 15 of these wells. No economic petroleum deposits were found, and all the wells were subsequently plugged and abandoned (NGDS, 2012). Two additional deep wells, one a geothermal test well (SunHub 25-1) and the other a recently drilled oil and gas exploration well (CPC 17-1) have also been drilled in the area (Table 1). Subsurface temperatures in the wells represent a mix of DSTs and/or BHTs.

Wireline logs in oil and gas wells are generally run soon after drilling, before thermal perturbations have dissipated (Cao et al., 1988a, b; Bullard, 1947; Deming, 1989; Edwards, 2013; Guyod, 1946; Henrikson, 2000; Henrikson and Chapman, 2002; Prensky, 1992). Drilling mud circulation tends to artificially cool the lower, and heat the upper, portions of the well bore, and the disturbances may take several months to dissipate (Beardsmore and Cull, 2001; Bullard, 1947; Guyod, 1946).

Numerous methods have been devised to correct for these thermal disturbances. Hermanrud et al. (1990) tested 22 methods developed between 1946 and 1988 against DST control data. Goutorbe et al. (2007), Crowell and Gosnold (2011), Crowell et al. (2012), and Edwards (2013) made similar comparisons of various methods. These studies showed that most methods reliably

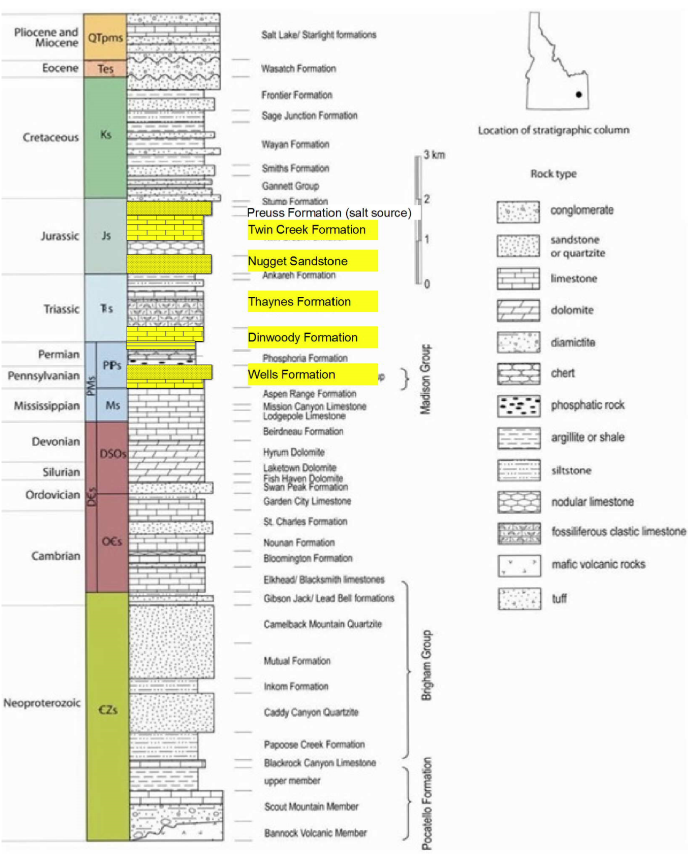

Figure 2. Composite lithostratigraphic column for the study area showing formations that may be sufficiently permeable to be productive reservoirs (yellow). Modified from Oriel and Armstrong (1971), Oriel and Platt (1980), and Long and Link (2007).

estimate formation temperatures to about ±10°C. Some methods are much more accurate, but also complex, and require data that are rarely available.

An evaluation of some of these methods was undertaken during this study, wherein corrected BHTs were compared against available DSTs, which are generally assumed to reflect in situ formation temperatures in recently drilled wells (Beardsmore and Cull, 2011; Förster and Merriam, 1995; Harrison et al., 1983; Hermanrud et al., 1990). The Henrikson (2000) and Henrikson and Chapman (2002) methods have been used with reasonable success to correct BHTs within the Great Basin (Allis et al., 2011, 2012; Gwynn et al., 2013; Edwards, 2013 - although the latter only used the Horner-type correction). These methods require accurate shut-in duration data. The depth-dependent methods evaluated include the equations of Kehle, as defined by Gregory et al. (1980); Harrison et al. (1983), as defined by Blackwell and Richards (2004); Förster and Merriam (1995), as revised by the SMU Geothermal Library and reported by Crowell et al. (2012); Morgan and Scott (2011); and Crowell et al. (2012). These methods were all derived in specific basins, and may not work well in other settings (Crowell and Gosnold, 2011; Crowell et al., 2012), which is why they were evaluated here.

In this relatively small dataset, the Horner and Henrikson methods tended to undercorrect slightly and the Morgan, Harrison (SMU-modified version), and Kehle methods tended to overcorrect slightly. The other methods overcorrected by a much larger margin with increasing depths. Since the more reliable methods were all roughly equal in the number of times that they correlated best with DST data, an average correction based on the Morgan, Harrison, and Henrikson/Horner (if shut-in time data were available) techniques was used. The final corrected temperatures (deepest only) are summarized in **Table 2**.

2.3. Corrected Geothermal Gradients

Geothermal gradients for each well were calculated using surface temperatures as determined in Welhan et al. (2014) and the deepest DST or corrected BHT. Most of the wells in this study also have intermediate-depth BHT and/or DST data, but since the temperatures define a fairly uniform and linear gradient (because thermal conductivity values throughout the well bore vary minimally), they do not significantly alter the calculated gradients shown in Table 2.

Table 1. Summary of deep wells with temperature data in the study area. Data extracted from http://www.idahogeology.org/services/Oilandgas/Table.asp.

API	Well Name	Operator	Latitude[1]	Longitude[1]	Surface Elevation (m)	Total Depth (m)	Spud Date	End Drilling Date
11-07-20019	Archie Parker No. 1	Texaco	42.30514	-111.45305	1882	3051	3-Jan-1988	19-Mar-1988
11-19-20003	Bald Mountain No. 1	Amoco Production Co.	43.10484	-111.20103	2495	2768	1-Aug-1983	5-Nov-1983
11-19-20004	Bald Mountain No. 2	Amoco Production Co.	43.10512	-111.22446	2370	4314	6-Jul-1981	18-Apr-1982
11-07-20008	Bennington No. 3-24	Ladd Petroleum	42.40377	-111.42060	2001	4124	5-Oct-1979	1-Mar-1980
11-07-20007	Big Canyon Federal No. 1-13	Union Texas Petroleum	42.54825	-111.37449	2070	3570	12-Sep-1978	15-Mar-1979
11-19-20001	Black Mountain Federal No.1	American Quasar Petroleum Co.	43.10924	-111.13688	2495	4368	17-Aug-1976	27-Mar-1977
11-29-00000	Dry Valley No. 1	Standard Oil of Calif.	42.77624	-111.33418	2060	2398	8-Jul-1952	5-Dec-1952
11-07-20013	Dunn's Canyon Federal No. 1-22	Chevron USA Inc.	42.45284	-111.30293	2134	4129	1-Dec-1980	17-Sep-1981
11-07-20012	Federal DI No. 1	Cities Service Co.	42.10327	-111.18099	1940	3128	10-Feb-1981	21-Jun-1981
11-29-20001	Federal Elk Valey No. 1	May Petroleum Inc.	42.53241	-111.09520	2284	1195	14-Jul-1976	19-Aug-1976
11-29-20004	Federal No. 1-8	May Petroleum Inc.	42.57053	-111.10517	2343	5105	15-Jul-1977	27-Sep-1978
11-19-20002	Gentile Valley No. 1-9	Continental Oil Co.	43.08935	-111.53288	2080	3021	20-Sep-1978	16-Aug-1979
11-19-00000	Government No. 1	Edwin Allday	43.39756	-111.21326	1699	1756	3-Sep-1965	1-Mar-1966
11-07-20006	Grace Federal No. 10-1	American Quasar of New Mexico	42.04858	-111.07010	2325	3615	21-Feb-1978	20-Aug-1978
11-11-20002	Hoff No. 1-8M	Union Oil Co. of Calif.	43.34336	-111.91790	1753	2726	22-May-1979	30-Oct-1979
11-29-20006	Idaho State "A" No. 1	Phillips Petroleum Co.	42.90278	-111.29906	2038	4963	12-Feb-1981	30-Sep-1982
11-07-20005	Jensen No. 22-1	American Quasar of New Mexico	42.27151	-111.30341	1812	3591	1-Sep-1977	27-Jan-1978
11-11-20001	King No. 2-1	American Quasar of New Mexico	43.27615	-111.61489	2012	4132	3-Feb-1978	22-Aug-1978
11-07-20010	N. Eden Federal No. 21-11	American Quasar	42.02776	-111.20460	2114	2862	24-Dec-1979	31-May-1980
11-07-20011	N. Rabbit Creek Federal No. 6-21	American Quasar	42.06598	-111.12355	2055	3537	19-Jan-1980	24-Jul-1980
11-07-20009	Rigby "A" Williams No. 1	Cities Service	42.25843	-111.09936	1899	3360	25-Oct-1979	5-Mar-1980
11-07-00000	Sheep Creek No. 1	Standard of Calif.	42.07952	-111.18723	1986	2063	24-May-1952	18-Dec-1952
11-19-20005	State No. 12-31	Juniper Petroleum Co.	43.29111	-111.58472	2057	2981	18-Jul-1981	16-Oct-1981
11-29-20005	Stoor "A" No. 1	Phillips Petroleum Co.	42.95347	-111.32313	2059	4605	23-Dec-1979	15-Jan-1980
11-07-20015	Sweetwater No. 5-13	Sohio Petroleum Co.	42.05552	-111.10904	2041	3541	2-Sep-1983	20-Jan-1984
11-19-20007	Tincup Mountain Federal No. 1	Sun Exploration and Production Co.	43.01061	-111.22467	2456	5060	19-Sep-1984	14-Jun-1985
11-19-00000	USA-TJ Weber No. 1-A	Pan American Petroleum	43.22928	-111.26237	2428	2962	29-Sep-1963	29-Oct-1964
11-29-00000	USA-Wild No. 1	Amerada Petroleum	42.52566	-111.08490	2285	1254	25-Aug-1963	13-Oct-1963
11-07-20016	Worm Creek No. 1	Murphy Oil	42.16149	-111.41771	1846	2284	17-May-1984	23-Jul-1984
11-19-20011	CPC 17-1	CPC Minerals, LLC	43.15767	-111.44868	1954	2885	1-Sep-2007	6-Dec-2001
11-29-30001	SunHub 25-1	Hunt Oil Co.	42.78670	-111.61170	1890	2373	5-Oct-1979	1-Mar-1980

[1] WGS 1984

Table 2. Summary of temperature, geothermal gradient, thermal conductivity, and heat flow data for deep wells in the BVF study area.

Well Name	Data Type	Corrected Temperature Depth (m)[1]	Corrected Temperature (°C)[2]	Surface Temperaure (°C)[3]	Overall Corrected Gradient (°C/km)[4]	Average Thermal Conductivity (W/m·K)[5]	Heat Flow (mW/m²)[6]	Modeled Heat Flow (mW/m²)[7]
Archie Parker No. 1	BHT	3041	87.0	7.6	26.1	3.1	81	75
Bald Mountain No. 1	BHT	2749	94.4	4.5	32.7	3.2	104	100
Bald Mountain No. 2	BHT	3832	140.0	4.5	35.4	2.6	91	85
Bennington No. 3-24	BHT	4127	97.3	6.9	21.9	2.8	62	50
Big Canyon Federal No. 1-13	BHT	3577	172.4	6.4	46.4	2.5	117	116
Black Mountain Federal No.1	BHT	4159	120.3	3.7	28.0	2.5	70	70
Dry Valley No. 1	BHT	1903	51.4	6.5	23.6	2.7	64	65
Dunn's Canyon Federal No. 1-22	BHT	4079	147.3	6.0	34.6	2.8	97	93
Federal DI No. 1	BHT	3056	80.6	7.2	24.0	2.6	62	60
Federal Elk Valey No. 1	BHT	967	36.8	5.0	32.9	2.8	93	93
Federal No. 1-8	BHT	5104	167.1	4.6	31.8	2.6	84	80
Gentile Valley No. 1-9	BHT	3008	161.8	6.3	51.7	2.6	136	129
Government No. 1	DST	405	21.1	8.8	30.4	2.7	82	67
Grace Federal No. 10-1	BHT	3616	85.2	4.8	22.2	2.7	61	58
Hoff No. 1-8M	BHT	2721	102.5	8.4	34.6	2.5	86	85
Idaho State "A" No. 1	BHT	4979	183.4	6.6	35.5	2.9	102	98
Jensen No. 22-1	BHT	3499	96.6	8.1	25.3	2.7	67	57
King No. 2-1	BHT	4069	202.2	6.8	46.9	2.4	114	107
N. Eden Federal No. 21-11	DST	3190	84.4	6.1	24.6	2.6	63	64
N. Rabbit Creek Federal No. 6-21	BHT	3538	87.5	6.5	22.9	2.7	63	59
Rigby "A" Williams No. 1	DST	3347	75.0	7.5	20.2	2.5	50	50
Sheep Creek No. 1	BHT	2053	56.2	6.9	24.0	2.6	62	57
State No. 12-31	BHT	2965	116.9	6.5	37.2	2.6	99	92
Stoor "A" No. 1	BHT	4510	192.4	6.5	41.2	2.3	95	91
Sweetwater No. 5-13	BHT	3538	88.3	6.6	23.1	2.9	68	64
Tincup Mountain Federal No. 1	BHT	5056	179.5	3.9	34.7	2.9	101	93
USA-TJ Weber No. 1A	BHT	2964	155.3	4.1	51.0	2.7	138	132
USA-Wild No. 1	DST	1229	50.6	5.0	37.1	2.6	98	91
Worm Creek No. 1	BHT	2284	58.5	7.8	22.2	2.4	53	50
CPC 17-1	BHT	2503	160.3	7.1	61.2	2.7	165	160
SunHub 25-1	BHT	2373	80.1	7.6	30.5	2.7	82	79

[1]Based on deepest releable corrected BHT or DST.
[2]Reliable corrected BHT or DST (see text).
[3]Mean annual surface temperature + 3°C (see text).
[4]Gradient based on deepest reliable corrected BHT or DST and calculated surface temperature.
[5]Average of thermal conducivity values used in geotherm models.
[6]Heat flow calculated by multiplying the average thermal conductivity and the overall geothermal gradient.
[7]Heat flow calculated using geotherm models.

2.4. Thermal Conductivity

Lithologic data of some sort were available for all wells of interest. With few exceptions, lithologic descriptions of geologic formations were gleaned from the NGDS database, although driller's logs, well reports, core reports, lithologic/mud logs, etc. were also used when necessary. Since no actual thermal conductivity data from these wells were available, values were estimated based on published averages for the lithologies reported in each well (Table 3).

For geologic formations with a single lithology (as described in the formation tops database; NGDS, 2012), the average thermal conductivity for that lithology was used, based on sources compiled by Beardsmore and Cull (2001). In the case of formations comprising several distinct lithologies, mud logs and other well data were used to estimate the relative proportions of each rock type and the overall thermal conductivity was calculated using the harmonic mean (Beardsmore and Cull, 2001) and then assigned to the formation (Table 3).

Lateral heterogeneities in the formation, differences in the sections of the formation penetrated by different wells, and perhaps errors in lithologic descriptions, resulted in differing estimates of the representative thermal conductivity in some formations. For example, thermal conductivity in the Woodside Shale, calculated using data from four wells, varied from 1.85 to 2.84 W/m·K, a difference leading to heat flow estimates of 125 to 142 mW/m² in the USA–T.J. Weber 1A well. An overall harmonic mean was used in this case, and data from multiple wells in most other formations varied less. In some wells the lithology of the upper 400–1100 m was not available, so data from the nearest well with complete lithologic data were used in these sections. The depth-averaged thermal conductivity for any given well in the study area ranges from 2.3 to 3.2 W/m·°K, with an aggregate average of 2.7 W/m·°K.

Table 3. Derived thermal conductivity estimates for sedimentary units in the study area, based on estimated proportions of lithologies and typical thermal conductivities for component lithologies as compiled by Beardsmore and Cull (2001). See text for procedure and assumptions.

Geologic Unit	Rank	Age	Lithology[1]	Estimated Unit Thermal Conductivity (W/m·K)2
Amsden	Formation	Pennsylvanian and Upper Mississippian	LS / CHT / SIS / SS / CGL	3.77
Ankareh	Formation	Upper Triassic	SH / LS	2.00
Belcher	Member	Lower Cretaceous	CGL / MS / SS	2.58
Bighorn	Formation	Upper Ordovician	DS	4.33
Black	Bed	Lower Triassic	SH	1.72
Boundary Ridge	Member	Middle Jurassic	SIS / LS	2.73
Brazer	Formation	Middle to Late Mississippian	LS	2.72
Death Canyon	Member	Middle Cambrian	LS	2.72
Dinwoody	Formation	Lower Triassic	LS / SIS	2.84
Eureka	Formation	Middle to Late Ordovician	QZT	5.63
Gannett	Group	Lower Cretaceous	MS / SS / CGL / LS /SH	2.84
Giraffe Creek	Member	Middle Jurassic	LS	2.77
Gypsum Springs	Member	Lower Jurassic	SIS / LS / CS	2.02
Leeds Creek	Member	Middle Jurassic	LS	2.72
Lodgepole	Formation	Lower Mississippian	LS	2.72
Madison	Formation	Upper and Lower Mississippian	LS	2.72
Nugget	Group	Lower Jurassic	SS	3.70
Park Sh	Formation	Middle Cambrian	SH / DS	1.83
Phosphoria	Formation	Permian	CHT	2.06
Preuss	Redbeds	Middle Jurassic	SIS / CS / HAL / GYP	2.98
Rich	Member	Middle Jurassic	LS	2.72
Salt Lake	Formation	Miocene - Pliocene	SIS / SS /CGL	2.39
Sliderock	Member	Middle Jurassic	LS	2.40
Stump	Formation	Upper and Middle Jurassic	SIS / SS / LS	2.60
Thaynes	Formation	Lower Triassic	LS / SIS	2.50
Three Forks	Formation	Mississippian and Upper Devonian	SH / SIS	4.06
Twin Creek	Formation	Middle Jurassic	LS / SIS	2.51
Wasatch	Formation	Lower Eocene	MS / SS / CGL / CHT	2.58
Watton Creek	Member	Middle Jurassic	LS	2.72
Wayan	Formation	Early Cretaceous	MS	1.95
Weber	Formation	Permian - Pennsylvanian	SS / SH / DS	3.11
Wells	Formation	Permian - Pennsylvanian	LS / SS / DS	3.75
Woodside	Formation	Lower Triassic	SH / SIS / SS / LS	2.16

CHT = Chert	GYP = Gypsum	QZT = Quartzite
CGL = Conglomerate	HAL = Halite	SS = Sandstone
CS = Claystone	LS = Limestone	SH = Shale
DS = Dolomite	MS = Mudstone	SIS = Siltstone

[1]Does not reflect relative proportions of each lithology or modifiers such as "calcareous shale" that might shift thermal conductivity away from typical values.

[2]See text for information on how average thermal conductivity was derived.

3. Heat Flow

Heat flow is the product of temperature gradient and thermal conductivity. The easiest way to calculate heat flow from well data is to simply multiply the geothermal gradient and the representative (mean) thermal conductivity for the entire well bore (Table 2). However, this method assumes a constant geothermal gradient, which is unrealistic unless thermal properties are homogeneous throughout the entire stratigraphic sequence (Gallardo and Blackwell, 1999).

Heat flow values for each well were also calculated by entering thermal conductivity data into geotherm models generated using a spreadsheet. These models calculate the temperature gradient over defined intervals (100 m) of thermal conductivity data. The input heat flow value can be adjusted to produce a temperature-depth profile throughout the entire well bore that intersects plotted temperature data. Heat flow values calculated with this method were usually slightly lower, but similar to those using the average gradient and thermal conductivity data (Table 2). The differences are generally small because many of the formations in the ITB have similar thermal conductivities, which result in fairly linear gradient profiles.

Calculating heat flow with geotherm models allows deflections in the temperature profile to be modeled, reflecting changes in lithology/thermal conductivity (Figure 4). The models may also highlight unreliable BHT or DST data in cases where there are temperatures at multiple depths that do not correlate well or where temperatures are unrealistically high or low. Faulty temperature data were identified in several wells using this approach. For example, three BHT measurements from the USA–T.J. Weber 1A well were corrected using the best available data. The deepest two appeared to be reliable once the appropriate thermal conductivities were entered into the geotherm model. However, the shallowest BHT value did not fit the resulting curve using any combination of reasonable thermal conductivity values, suggesting that the BHT value was incorrectly measured or reported. Similarly, the models helped show that in most wells the averaged BHTs from several correction methods correlated better with DST data than BHTs corrected by a single method.

The temperature profile in a well may also be modified by advective heat transport in the penetrated rock, either at specific depths or over the entire depth. Advective effects, especially within localized zones, can make geotherm model fitting problematic since temperature profile deflections may not be caused solely by thermal conductivity changes (Lachenbruch and Sass, 1977; Sass and Walters, 1999). Since temperature data generally plot fairly linearly for the ITB wells, we assume the thermal regime to be generally conductive. As such, the temperature-depth plots and, to a lesser extent (due to uncertainty in thermal conductivities), the heat flow calculations are believed to be reasonable. However, variability in thermal gradients and heat flow on a localized scale does suggest the possibility of advective effects in some wells.

Subsurface compaction tends to increase thermal conductivity as porosity decreases. These effects were not calculated for this study. Therefore, thermal conductivity estimates (and corresponding heat flow) may be slightly higher at depth, so heat flows in Table 2 may be biased slightly towards more conservative minimum values. In any event, the effects of compaction would likely be obscured by uncertainties in the BHT and thermal conductivity data. Despite uncertainties in heat flow estimates due to compaction or advection, it should be remembered that the temperatures (± 10°C) plotted in Figure 4 represent corrections to actual observations.

4. Spatial Context of Subsurface Temperatures and Pore Fluids

4.1. Geothermal Gradients

Figure 5 summarizes all heat flow estimates derived in this study together with best available heat flow estimates from the SMU database (SMU, 2008) and heat flow data derived from recent shallow thermal gradient drilling in the study area (Welhan, 2014).

To impose some geographic specificity on the discussion of heat flow results and subsurface temperatures, the temperature-depth curves shown in Figure 4 were grouped into the five zones shown in Figure 5 in order to identify the most prospective areas for further investigation.

Zone 1: This zone is marginal with respect to the temperature-depth target of >150°C at 3–4 km depth defined by Allis et al. (2013) and Holbrook et al. (2014) and refined by Allis and Moore (2014). Only three wells were drilled in this zone, so data were

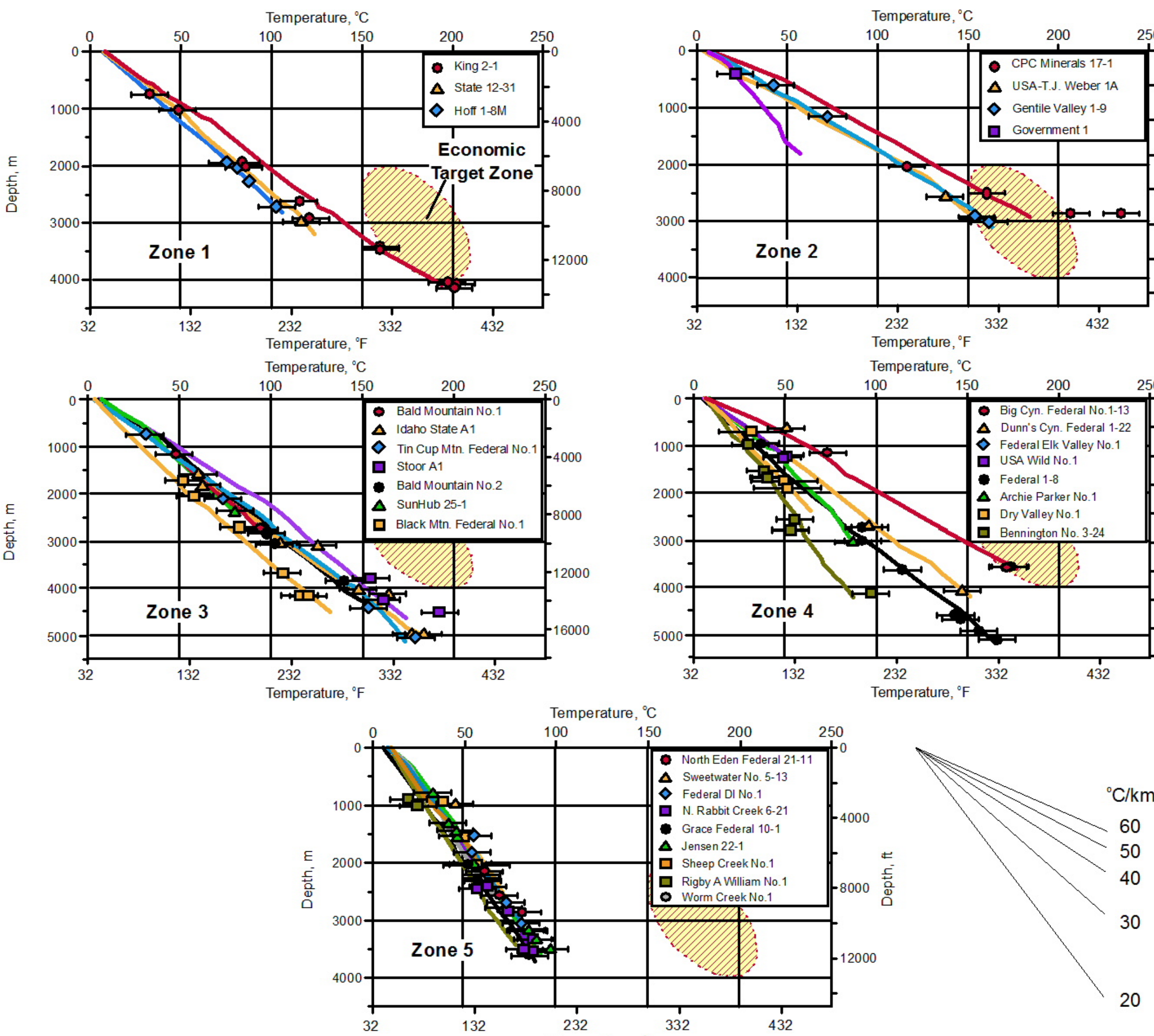

Figure 4. Modeled temperature-depth profiles (geotherms) for 31 deep wells within the study area. Models used DST and corrected BHT data together with inferred thermal conductivities of lithologic units in 100 m intervals to estimate surface heat flow and geothermal gradients. Zones 1-5 refer to areas shown in Figure 5. Shaded ellipses indicate target temperature and depth range defined by Allis and Moore (2014) for drilling in hot sedimentary basins.

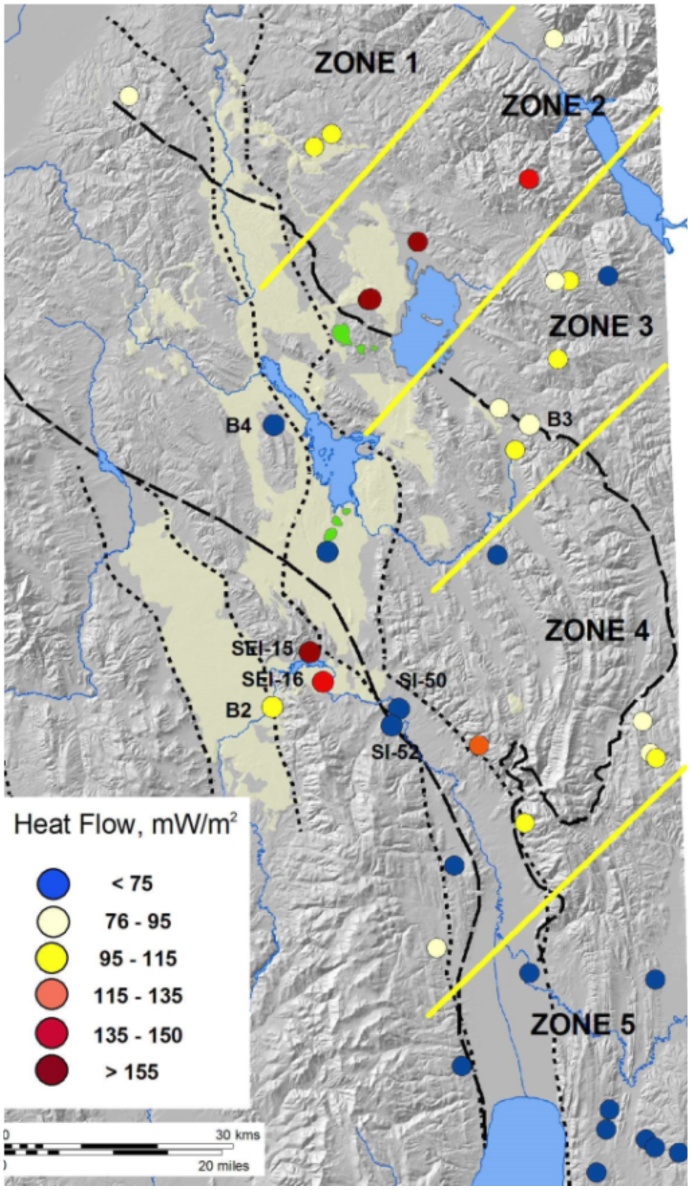

Figure 5. All available heat flow estimates in the study area. Labeled wells (SI-, SEI-) represent shallow heat flow estimates from SMU's (2008) database as reconciled with heat flow measurements in new thermal gradient wells (B2, B3, B4). All other wells are those evaluated in this study (Figure 3 and Table 1). Other map symbology is the same as in Figure 1. Wells are grouped into five zones to identify areas with the highest geothermal potential (Zone 2, part of Zone 1, and possibly the Big Canyon 13-1 well in Zone 4), as well as areas with little or no potential (Zone 5).

limited, and of those only the King 2-1 well revealed temperatures in the target zone.

Zone 2: From a thermal standpoint this zone shows the most potential. The thermal gradients in three wells are similar and reach target temperatures at depths of 2500–3000 m, well within the economic target zone. The two deepest/highest temperatures in the CPC 17-1 well (Figure 4) do not correlate well with the shallower temperatures and yield a heat flow of 210 mW/m² in the geotherm model. There is no obvious error in the data, judging from the log headers, but there is reason to suspect the reliability of these temperature measurements, particularly since there is a 28°C difference between them at nearly identical depths. No other data are available to determine the accuracy of either of these BHTs. If one or both of these temperature values is indeed correct, then advective overprinting by upflowing high-temperature fluids may be responsible.

The only temperature data available for the Government No. 1 well came from a DST measurement and is probably reliable. If the thermal conductivity estimates are accurate, the estimated thermal gradient is low compared to other wells in this zone, suggesting that the thermal anomaly may not extend this far to the northeast.

Zone 3: Thermal gradients in this zone are generally uniform but are too low to encounter target temperatures at economic depths.

Zone 4: Thermal gradients here are the most variable and, with one exception, are not sufficient to intersect the economic target zone. However, the Big Canyon Federal No. 1-13 well, which has an average gradient of about 46°C/km, does meet the thermal criterion. This well is located 15 km from the Sulfur Springs acid-sulfate area that lies about 7 km east of the city of Soda Springs. Although this area of acid ground is not warm, it is known to be the location of a vigorous CO_2 flux (Lewicki et al., 2012). A stratigraphic or other localized effect may promote higher temperatures at shallower depth in this well and/or greatly decreased temperatures in surrounding wells. The high heat flow and gradient observed in the Big Canyon Federal No. 1-13 well are worthy of further study.

Zone 5: This zone is characterized by very uniform low gradients on the order of 23°C/km as along with low heat flow. As such, this area likely has low geothermal potential.

4.2. Saline Geothermal Fluids

Welhan et al. (2014) summarized a total of 26 chemical analyses on fluids sampled in DSTs representing 12 DST intervals in six wells[2] over a depth range of 326 to 4176 meters. The stratigraphic positions of these fluids are shown in Figure 6, color-coded for the total dissolved solids (TDS) concentration of the least-diluted sample in each DST interval.

Hot, saline fluids occur over a depth range of several km and over a wide geographic area. All are sodium-chloride (Na-Cl) fluids ranging from almost pure Na-Cl brine of up to 320 grams/liter TDS to mixed Na-Cl-SO_4 fluids with TDS as low as 11 grams/liter, indicating they derive from dissolution of halite in the Preuss Sandstone together with minor amounts of gypsum and/or anhydrite reported from a range of stratigraphic units in the area (Welhan at al., 2014). Multiple samples collected from the same DST interval display considerable variability in their salt content, indicating that varying degrees of dilution may explain the differences in maximum salinities observed between wells and DST intervals, but in situ variations in formation fluid salinities may be present in all or some DST intervals.

Several trends in Figure 6 are apparent: (1) decreasing-upward salinities exist in wells where multiple intervals were sampled over a wide range of depths (King 2-1 and Idaho State A No.1); (2) high-salinities occur as far as 3 km below the Preuss redbeds in the four northernmost wells; and (3) the southernmost two wells (Jensen No. 22-1 and North Eden Federal No. 21-11) did not encounter the Preuss Sandstone and its salt beds and also have the lowest salinities. These observations are consistent with the

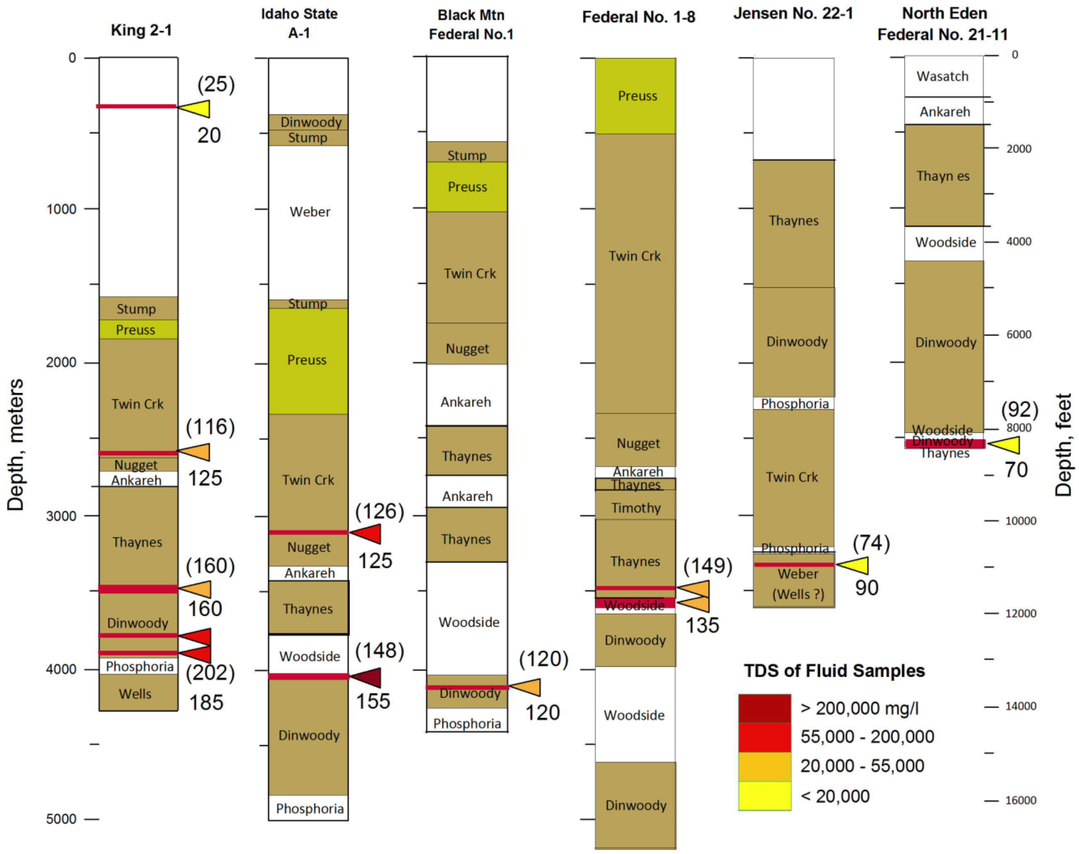

Figure 6. All DST intervals (arrowheads) in which hot, saline fluids were sampled; northernmost wells are on the left; southernmost wells, on the right. Refer to Figure 3 for well locations. All fluids are of Na-Cl composition with 1:1 molar Na:Cl and minor, variable amounts of sulfate (Welhan et al., 2014). Total dissolved solids (TDS) concentrations are plotted with a color-coded scale representing the least-diluted fluid samples in each DST interval. Numeric entries in parentheses represent measured DST temperatures; otherwise, corrected BHTs or modeled geotherm temperatures (°C) are shown. Formations with potentially higher permeability are indicated in brown and halite source beds are in the Preuss (green).

hypothesis that circulating hydrothermal fluids encroaching on salt-rich intervals in the Preuss Sandstone are dissolving its salt.

Hydrothermally driven salt dissolution could have significant implications for how heat is stored and/or redistributed in the stratigraphic section. To illustrate, assume that brine with a salinity of 180 grams/liter (mid-range of 26 DST samples), generated within a 40-m thick halite bed (the average thickness of halite in these wells), sinks into the underlying stratigraphic section via density flow and allow for further salt dissolution by encroaching hydrothermal fluids. A simple salt balance shows that the mass of dissolved salt redistributed into the underlying 3 km of stratigraphic section in this manner could generate secondary porosities of the order of 20-40 percent in the Preuss salt, similar to porosities generated during solution-mining of underground evaporite deposits (Sanford, 1996). Generation of cavernous porosity could also explain the characteristic swarming nature of microseismicity in the study area, as collapsing caverns generate new fracture permeability in the Preuss salt beds (Welhan et al., 2014).

Finally, it should be noted that the process of density-driven redistribution of hot brine could have important implications for how heat is stored in this geologic setting. Fluid rising from the magmatic heat source via thermal buoyancy is capable of dissolving large quantities of the salt because the solubility of halite at 200 °C is not significantly different than its solubility at room temperature. As increasing brine salinity overcomes thermal buoyancy, these hot dense brines would sink into underlying stratigraphic reservoirs that can be vertically and laterally quite distant from the salt source.

Such a mechanism could also effectively "insulate" the deeper thermal reservoir against conductive heat loss in a manner analogous to how a solar pond stores heat in its deepest, highest salinity layers (RMIT, 2014). For example, the sharp rise in corrected temperatures observed in Idaho State A1 (from 105 °C at 3000 m to 125°C at 3100 m; Figure 4, Zone 3) and the "kink" in its modeled temperature profile may not be due to advective overprinting but could reflect storage of hot, denser brine that has accumulated at deeper stratigraphic levels. In this well and nearby Stoor A1 (the two hottest wells in Zone 3), Preuss salt occurs at depths of 2000 to 2800 m, respectively, just above where the marked temperature change occurs. Hot brine generated in the Preuss salt beds and redistributed vertically in the underlying section would tend to flatten the thermal gradient where downward flow of brine occurs and steepen the thermal gradient where brine "ponding" occurs. CPC Minerals 17-1's extreme BHTs, if reliable, may be an example of the latter, where brines generated in the Preuss Sandstone at ca. 2400 m accumulate at depths near 2800 m; alternatively, a zone of lost circulation in the highly fractured Twin Creek limestone at ca. 2600 meters could be a direct conduit for high-temperature fluids to enter this part of the sedimentary section.

Judging from the large vertical interval over which hot saline fluids are found in this area (Figure 6), the impact of vertical heat redistribution by thermohaline flow should be evaluated to determine whether it can sequester high-enthalpy fluid over a much larger stratigraphic interval than the presumably restricted zones where hydrothermal circulation accesses the salt-bearing strata.

5. Conclusions

A number of common correction methods were applied to BHTs from 31 deep wells in the western ITB and were compared to DST temperatures believed to be reliable. Several correction methods produced erroneous results, most likely because they were calibrated in a different geologic setting. In contrast, the Harrison, Kehle, Morgan, Henrikson, and Horner corrections all provided reasonable results with only minor variations at depth. A composite average of corrected temperatures based on methods other than the Kehle method was calculated for each BHT and, in most cases, brought the resulting corrected temperature closer to the DST data. The corrected BHT and DST data were then combined with estimated thermal conductivity values to calculate heat flow at each well.

Our evaluation represents the most detailed analysis of temperature and heat flow data in the ITB to date. Based on the results, two areas were identified as having the best potential for geothermal development. The first is Zone 2 in the vicinity of the Gentile Valley 1-9, CPC Minerals 17-1, and USA-T.J. Weber 1-A wells and, based on the heat flow of the King 2-1 well, the adjacent section of Zone 1. In total, heat flows and gradients found in Zone 1 shw it to be marginally suitable based on the temperature-depth targets defined by Allis and Moore (2014), Allis et al. (2011, 2012, 2013) and Holbrook et al. (2014) for hot sedimentary basin geothermal development. The second is what appears to be a very localized area around the Big Canyon Federal No. 1-13 well in Zone 4.

A large part of the study area appears to be characterized by hot brines and saline formation fluids at depths of 3 to 5 km. Whether these fluids play an important role in the development and/or spatial extent of the geothermal resource remains to be seen. However, sufficient circumstantial evidence exists that the hypothesis of vertical redistribution of heat within the stratigraphic section by density-driven flow of hot brines generated in the Preuss needs to be taken seriously. If high-enthalpy fluid is sequestered over a much larger stratigraphic interval than simply where active hydrothermal circulation takes place, this redistribution of heat would have significant implications for how these hot sedimentary reservoirs developed and how their heat can best be extracted sustainably.

6. Recommendations for Further Study

Although this study evaluated only Idaho well data, additional studies could be undertaken to examine the large amount of well data across the border in Wyoming.

Samples of cuttings (and some core) are available for several wells in the study area. Thermal conductivity testing on even a small number of samples would promote refinement of the estimated thermal conductivities (and heat flows) reported in this study and the cores could also provide vital data on porosity and permeability characteristics of potential reservoir rocks.

Systematic or "pattern" drilling of thermal gradient wells for geothermal exploration has been successfully used by a number of companies in the Great Basin (Young et al., 2012). Experience in the study area suggests that thermal gradient boreholes as deep as 250 m would greatly refine our understanding of the local thermal regime. Logical targets for drilling would be in Zone 2, parts of Zone 1, and in the area around the Big Canyon Federal No. 1-13 well in Zone 4.

Other exploration methods described by Jennejohn (2009) and Young et al. (2012) may also be beneficial. A cost-benefit analysis of such methods could be undertaken to identify the optimal spatial scales and target areas in which they can best be applied. Additional work in the study area has commenced using a play-fairway approach common to the oil and gas exploration industry. That project will combine geothermal expertise with extensive oil and gas exploration experience in play-fairway techniques with the objective of minimizing exploration risk for the geothermal industry.

The hydrodynamic impacts of thermohaline flow should also be evaluated within the context of hydrothermally facilitated dissolution of evaporites to determine whether it could be an important mechanism for sequestering high-enthalpy fluids in the sedimentary section, whether for conventional or EGS-based heat extraction.

Acknowledgements

This work was generously funded by the Geothermal Technologies Program of the U.S. Department of Energy (Award Numbers: UT-EE0002850 and ID-EE0002850). This paper is part of a project titled: "Novel Geothermal Development of Sedimentary Basins in the United States," Moore, J.N., and Allis, R.G. (co-Principal Investigators), which is partially funded by the Geothermal Technologies Program of the U.S. Dept. of Energy (Award DE-EE0005128).

References

Allis, R., Blackett, B., Gwynn, M., Hardwick, C., Moore, J., Morgan, C., Schelling, D., and Sprinkel, D., 2012. "Stratigraphic reservoirs in the Great Basin - the bridge to development of enhanced geothermal systems in the U.S." Geothermal Resources Council *Transactions*, v. 36, p. 351-357.

Allis, R., and J. Moore, 2014. "Can deep stratigraphic reservoirs sustain 100 MWe power plants?" Geothermal Resources Council *Transactions*, v. 38 (this volume).

Allis, R., Moore, J., Anderson, T., Deo, M., Kirby, S., Roehner, R., and Spencer, T., 2013. "Characterizing the power potential of hot stratigraphic reservoirs in the Western U.S." Thirty-Eighth Workshop on Geothermal Reservoir Engineering, *Proceedings*, Stanford University, SGP-TR-198, 9 pp.

Allis, R., Moore, J., Blackett, R., Gwynn, M., Kirby, S., and Sprinkel, D. S., 2011. "The potential for basin-centered geothermal resources in the Great Basin." Geothermal Resources Council *Transactions*, v. 35, p. 683-688.

Armstrong, F.C., 1969. "Geologic map of the Soda Springs Quadrangle, southeastern Idaho." U.S. Geological Survey *Misc. Geologic Investigations Map* I-557, scale 1:48,000, 2 sheets. http://pubs.er.usgs.gov/publication/i557

Armstrong, F.C. and S.S. Oriel, 1965. "Tectonic development of Idaho-Wyoming thrust belt." Am. Asoc. Petroleum Geologists *Bulletin*, v. 49, p. 1847-1866.

Beardsmore, G. R., and Cull, J. P., 2001. "Crustal heat flow: a guide to measurement and modeling." Cambridge University Press, 334 pp.

Blackwell, D.D., 1983. "Heat flow in the northern Basin and Range province" *in* The Role of Heat in the Development of Energy and Mineral Resources in the Northern Basin and Range Province; Special Report 13, edited by Geothermal Resources Council, 81 pp.

Blackwell, D.D., and M. Richards, 2004. "Calibration of the AAPG geothermal survey of North America BHT database." AAPG Meeting, Dallas, Texas, April 2004, Southern Methodist University Geothermal Lab poster on BHT calibration, URL: http://smu.edu/geothermal/BHT/BHT.htm

Blackwell, D.D. and co-workers, 2011. "Heat flow map of the conterminous United States." http://Google.org/egs.

Bullard, E. C., 1947. "The time necessary for a borehole to attain temperature equilibrium." Geophysical Journal International, v. 5, p. 127-130. doi: 10.1111/j.1365-246X.1947.tb00348.x

Cao, S., Lerche, I., Hermanrud, C., 1988a. "Formation temperature estimation by inversion of borehole measurements." Geophysics, v. 53, no. 7, p. 978-988.

Cao, S., Lerche, I., Hermanrud, C., 1988b. "Formation temperature estimation by inversion of borehole measurements, Part II: Effects of fluid penetration on bottom-hole temperature recovery." Geophysics, v. 53, no. 10, p. 1347-1354.

Christiansen, E.H., M.F. Sheridan and D.M. Burt, 1986. "The Geology and Geochemistry of Cenozoic Topaz Rhyolites from the Western United States." Geol. Soc. Am. *Special Paper* 205, 82 pp.

Crowell, A. M., and Gosnold, W. D., 2011. "Correcting Bottom-Hole Temperatures: A Look at the Permian Basin (Texas), Anadarko and Arkoma Basins (Oklahoma), and Williston Basin (North Dakota)." "Geothermal Resources Council *Transactions*, v. 35, p. 735-738.

Crowell, A. M., Ochsner, A. T., and Gosnold, W. D., 2012. "Correcting Bottom-Hole Temperatures in the Denver Basin: Colorado and Nebraska." Geothermal Resources Council *Transactions*, v.36, p. 201-206.

Deming, D., 1989. "Application of bottom-hole temperature corrections in geothermal studies." Geothermics, v.18, no. 5-6, p.775-786.

Dixon, J.S., 1982. "Regional structural synthesis, Wyoming Salient of western overthrust belt." American Association of Petroleum Geologists *Bulletin* v. 66, p. 1560-1580.

Edwards, M.C., 2013. "Geothermal resource assessment of the Basin and Range Province in western Utah." U. of Utah M.S. Thesis, 113 pp.

Ford, M.F., 2005. "The petrogenesis of Quaternary rhyolite domes in the bimodal Blackfoot volcanic field, southeastern Idaho." Idaho State University M.S. thesis, 133 pp.

Förster, A., and Merriam, D. F., 1995. "A bottom-hole temperature analysis of the American midcontinent (Kansas): Implications to the applicability of BHTs in geothermal studies. International Geothermal Association, World Geothermal Congress (Florence, Italy) *Proceedings*, v. 2, p. 777-782.

Gallardo, J. and Blackwell, D. D., 1999. "Thermal structure in the Anadarko Basin." Am. Assoc. Petroleum Geologists *Bulletin*, v. 83, no. 2, p. 333-361.

Goutorbe, B., Lucazeau, F., and Bonneville, A., 2007. "Comparison of several BHT correction methods-a case study on an Australian data set." Geophys. J. Int. 170 (2): 913-922.

Gregory, A. R., Dodge, M. M., Posey, J. S., and Morton, R. A., 1980. "Volume and accessibility of entrained (solution) methane in deep geopressured reservoirs-Tertiary formations of the Texas Gulf Coast." U.S. Dept. of Energy DOE/ET/11397-1, pp. 361, OSTI # 5282675.

Guyod, H., 1946. "Temperature Well Logging (seven-part series)." Oil Weekly, v. 123 No. 8-11 and v. 124, no. 1-3, 47 pp.

Gwynn, M.; Blackett, B.; Allis, R., and Hardwick, C., 2013. "New geothermal resource delineated beneath Black Rock Desert, Utah." Thirty-Eighth Workshop on Geothermal Reservoir Engineering, *Proceedings*, Stanford University, SGP-TR-198, 9 pp.

Harrison, W.E., K.V. Luza, M.L Prater, and P.K. Chueng, 1983. "Geothermal resource assessment of Oklahoma." Oklahoma Geological Survey *Special Publication* 83-1, 42 pp.

Henrikson, A., 2000. "New heat flow determinations from oil and gas wells in the Colorado Plateau and Basin and Range of Utah." U. of Utah M.S. Thesis, 69 pp.

Henrikson, A. and D.S. Chapman, 2002. "Terrestrial heat flow in Utah." University of Utah unpubl. report, http://geology.utah.gov/emp/geothermal/pdf/terrestrialhf.pdf

Hermanrud, C., Cao, S., and Lerche, I., 1990. "Estimates of virgin rock temperature derived from BHT measurements: Bias and error." Geophysics, 55(7), p. 924-931.

Holbrook, J., Moore, J. N., Elsworth, D., Block, K. A., Allis, R., and Einstein, H., 2014. "An opportunity of geothermal proportions in sedimentary basins." The Sedimentary Record, v. 12, no. 1, p. 4-9.

IDWR, 1980. "Geothermal Resources of Idaho; Part 9." Idaho Dept. of Water Resources *Water Information Bull*. No. 30, Plate 1; 1:500,000 scale map.

Jennejohn, D., 2009. "Research and development in geothermal exploration drilling, Geothermal Energy Association, 25 pp.

Lachenbruch, A.H., and Sass, J.H., 1977. "Heat flow in the United States and the thermal regime of the crust" *in* J. G. Heacock (ed.), The Earth's crust. American Geophysical Union *Geophysics Monogram* 20, p. 625-675.

Lachenbruch, A.H., J.H. Sass and P. Morgan, 1994. "Thermal regime of the southern Basin and Range province; Implications of heat flow for regional extension and metamorphic core complexes." Journal of Geophysical Research, v. 99, p. 22121-22133.

Lewicki, J.L., G.E. Hilley, L. Dobeck, T.L. McLing, B.M. Kennedy, M. Bill and B.D.V. Marino, 2012. "Geologic CO_2 input into groundwater and the atmosphere, Soda Springs, ID, USA." Chem. Geology, v.339, p. 61-70.

Long, S.P., and P.K. Link, 2007. "Geologic map compilation of the Malad City 30 x 60 minute quadrangle, Idaho." Idaho Geological Survey *Technical Report* 07-1, scale 1:100,000.

McCurry, M. and J.A. Welhan, 2012. "Do Magmatic-Related Geothermal Energy Resources Exist in Southeast Idaho?" Geothermal Resources Council *Transactions*, v. 36, p. 699-707.

Mitchell, J.C., L.L. Johnson and J.E. Anderson, 1980. "Potential for Direct Heat Application of Geothermal Resources, Plate 1; Geothermal Investigations in Idaho, Part 9." Idaho Dept. Water Resources *Water Information Bull.* 30, 396 pp.

Morgan, P. and Scott, B., 2011. "Bottom-hole temperature data from the Piceance Basin, Colorado: Indications for prospective sedimentary basin EGS resources." Geothermal Resources Council *Transactions*, v. 35, p. 477-485.

NGDS, 2012. "Idaho-specific geothermal data." AASG Geothermal Data Repository, National Geothermal Data Sytem, http://repository.stategeothermaldata.org/repository/browse/

Oriel, S. S., and Armstrong, F. C., 1971. "Uppermost Precambrian and Lowest Cambrian Rocks in Southeastern Idaho." U.S. Geological Survey *Professional Paper* 394, 52 p.

Oriel, S.S. and L.B. Platt, 1980. "Geologic map of the Preston 1ox2o quadrangle, southeastern Idaho and western Wyoming." U.S. Geological Survey *Misc. Geologic Investigations Map* I-1127, scale 1:250,000. http://pubs.er.usgs.gov/publication/i1127

Prensky, S., 1992. "Temperature measurements in boreholes: An overview of engineering and scientific applications." The Log Analyst, v. 33, no. 3, p. 313-333.

Ralston, D.R. and A.L. Mayo, 1983. "Thermal ground water flow systems in the thrust zone in southeastern Idaho." U.S. Dept. of Energy, DOW/ET/28407-4 (DE84011598), 336 pp., one plate.

Ralston, D.R. and R.E. Williams, 1979. "Groundwater flow systems in the western phosphate field in Idaho." J. Hydrology, v. 43, pp. 239-264.

Ralston, D.R., J.L. Arrigo, J.V. Baglio, L.M. Coleman, J.M. Hubbell, K. Souder and A.L. Mayo, 1983. "Thermal ground water flow systems in the thrust zone of southeastern Idaho." U.S. Dept. of Energy DOE/ET/28407-4 (DE84011598), 336 pp.

RMIT, 2014. "Solar Pond Project: Innovative technology to collect solar energy for heating purposes." RMIT University, Melbourne, Australia, http://www.rmit.edu.au/browse;ID=905wa9169827.

Royse, F.M., Jr., 1993. "An overview of the geologic structure of the thrust belt in Wyoming, northern Utah and eastern Idaho" *in* Snoke, A.W., J.R.

Steidtmann, and S.M. Roberts (eds.), Geology of Wyoming, Geological Survey of Wyoming *Memoir* No. 5, p. 272-311.

Sanford, K.F., 1996. "Solution salt-mining in New York." Northeastern Geology and Environmental Sciences, v. 18, p. 97-107.

Sass, J. H., and Walters, M. A., 1999. "Thermal regime of the Great Basin and its implications for enhanced geothermal systems and off-grid power." Geothermal Resources Council *Transactions*, v. 23, p. 211-218.

Smith, R.L. and H.R. Shaw, 1979. "Igneous-Related Geothermal Systems *in* L.J.P. Muffler (ed.) Assessment of Geothermal Resources of the United States—1978, U.S. Geological Survey *Circ.* 790, p.10-17.

SMU, 2008. "Southern Methodist University Geothermal Laboratory heat flow database." http://smu.edu/geothermal

Welhan, J.A., 2014. "Final Heat Flow Deliverables for Supplemental Drilling Project; Final Report, prepared for NGDS Supplemental Drilling Project (U.S. Dept. of Energy Project ID-EE0002850) http://www.idahogeology.org/Geothermal/TGHDrillingProject/FinalReport-TGHDrillingProject/Deliverable%201-FinalSupplementalProjectReport.docx

Welhan, J.A., D. Garwood, and D. Feeney, 2013. "The Blackfoot Volcanic Field, Southeast Idaho: A Hidden High-T Geothermal Resource Revealed Through Data Mining of the National Geothermal Data Repository." Geothermal Resources Council *Transactions*, v.37, pp.365-374.

Welhan, J.A., M.L. Gwynn, S. Payne, M.O. McCurry, M. Plummer and T. Wood, 2014. "The Blackfoot Volcanic Field, Southeast Idaho: A Hidden High-Temperature Geothermal Resource in the Idaho Thrust Belt." Thirty-Ninth Workshop on Geothermal Reservoir Engineering *Proceedings*, Stanford University, Stanford University SGP-TR-202, 13 pp.

Young, K., Reber, T., and Witherbee, K., 2012. "Hydrothermal exploration best practices and geothermal knowledge Exchange on OpenEI." Thirty-Seventh Workshop on Geothermal Reservoir Engineering Proceedings, Stanford University, SGP-TR-194, 13 pp.

---

[1] http://www.idahogeology.org/Services/OilAndGas/Default.asp

[2] Idaho State A No.1; King No. 2-1; Black Mountain Federal No. 1; Federal No. 1-8 (Elk Valley #2); North Eden Federal 21-11; and Jensen 22-1. Refer to Figure 3 for well locations.